Journal of Aircraft

VOLUME 5 MARCH-APRIL 1968 NUMBER 6

# Investigation of Tilt-Rotor VTOL Aircraft Rotor-Pylon Stability

H. Kipling Edenborough*
*Bell Helicopter Company, Fort Worth, Texas*

**Rotor-pylon stability tests were conducted with the Bell XV-3 tilt-rotor convertiplane in the NASA Ames 40- × 80-ft tunnel. These tests, preceded by extensive analytical and dynamically scaled model work, were made to establish the validity of newly developed theoretical methods and to demonstrate rotor-pylon stability at high speed. Confirmation of predicted effects of various parameters was obtained. Operation at maximum tunnel speed was demonstrated with a number of different configurations. This investigation was initiated after a low-frequency rotor-pylon instability was encountered during full-scale tunnel tests in 1962. An analytical solution was developed through theoretical investigations, which were performed in conjunction with dynamically scaled model tests, each being used to guide the other. Isolation of the major parameters and determination of their effect on stability resulted from this work. Also, a physical understanding of the phenomenon, and simple means for providing stability were obtained. The latter include rotor control system coupling with pylon motion, increased pylon stiffness, and rotor flapping restraint. Validation of the effect of those as well as other parameters on rotor-pylon stability was obtained during the tunnel tests. This paper provides background information relevant to the tilt rotor-pylon stability problem, presents and discusses the full-scale test results, and shows the correlation between experimental and theoretical data.**

## Nomenclature

$a_1$ = rotor longitudinal flapping, rad
$b_1$ = rotor lateral flapping, rad
$C_{\phi x}$ = pylon pitch damping coefficient, ft-lb/rad/sec
$C_{\phi y}$ = pylon yaw damping coefficient, ft-lb/rad/sec
$C_{wb}$ = effective wing beam damping coefficient, lb/fps
$D$ = rotor diameter, ft
$h$ = pylon mast length, ft
$\Delta H$ = increment in blade element inplane force, lb
$I_b$ = blade flapping inertia, slug-ft$^2$
$J$ = propeller advance ratio
$K_b$ = rotor flapping restraint per blade, in.-lb/deg
$K_{\text{eff}}$ = effective pylon pitch spring rate including wing torsion, ft-lb/rad
$K_{wb}$ = effective wing beamwise spring rate, lb/ft
$K_x$ = longitudinal swashplate-pylon coupling ratio; 0 if swashplate locked to mast, 1 if fixed in space
$K_y$ = lateral/yaw swashplate-pylon coupling ratio
$K_{\phi x}$ = pylon pitch spring rate, ft-lb/rad
$K_{\phi y}$ = pylon yaw spring rate, ft-lb/rad
$\Delta L$ = blade element incremental lift, lb
$M_H$ = pylon pitching moment caused by inplane rotor force, ft-lb
$R$ = rotor radius, ft
$\bar{R}$ = effective rotor radius; $\frac{3}{4}R$, ft
$T$ = thrust, lb
$\Delta T$ = blade element incremental thrust, lb
$U$ = total airflow at blade element, fps
$V$ = freestream velocity, fps
$x_b, y_b, z_b$ = coordinates fixed in rotor (see Fig. 4)
$X, Y, Z$ = coordinates fixed in space (see Fig. 4)
$\Delta\alpha$ = blade element incremental angle of attack, rad
$\beta$ = blade flapping angle with respect to mast, rad
$\delta_3$ = rotor pitch-flap coupling ratio, rad
$\epsilon$ = azimuth phase angle for swashplate-pylon coupling, positive when swashplate indexed counter to direction of rotor rotation, deg
$\phi_o$ = rotor inflow angle, rad
$\phi_x$ = pylon pitch angle, rad
$\phi_y$ = pylon yaw angle, rad
$\psi$ = blade azimuth angle, rad
$\Omega$ = rotor angular velocity, rad/sec
$\omega_\beta$ = rotating blade natural undamped frequency
$\omega_x$ = pylon pitch natural frequency, cps
$\omega_y$ = pylon yaw natural frequency, cps
$(\dot{})$ = first time derivative of variable indicated

Presented as Paper 67-17 at the AIAA 5th Aerospace Sciences Meeting, New York, N. Y., January 23–26, 1967; submitted February 14, 1967; revision received December 11, 1967. The author wishes to acknowledge the numerous contributions to this program made by members of NASA and Bell Helicopter Company. Particular acknowledgment is given to M. Kelly, D. Koenig, and D. Hickey of NASA Ames and to E. Covington, E. Hall, C. Leibensberger, R. Lynn, M. Paine, and R. Smith of Bell.

* Assistant Project Engineer, Model 266 Composite Aircraft Test Programs.

## Introduction

THE XV-3 (Fig. 1) was designed and built in 1953–1955 under joint Army-Air Force sponsorship. Comprehensive flight and wind-tunnel test programs were conducted through 1962 by Bell, the Air Force, and NASA, accumulating approximately 500 hr of ground, flight, and tunnel test time.


**Fig. 1 XV-3 tilt-rotor VTOL in flight.**

Those test programs, discussed in Refs. 1–5, established the tilt-rotor concept as a practical solution to VTOL, combining the efficient hovering and low-speed characteristics of the helicopter with the increased speed capability of the fixed wing.

Detailed flight test results indicated that rotor transient flapping in certain airplane maneuvering conditions became high, and that the classical short-period airplane oscillation decreased in damping as speed was increased. As rotor pitch-flap coupling (delta-three) acts to reduce flapping through its effect on blade feathering, full-scale wind-tunnel tests were performed in 1962 at the NASA Ames 40- × 80-ft tunnel to evaluate the over-all effect of delta-three on rotor-pylon behavior at high advance ratios. At a tunnel speed near 130 knots, a sustained rotor-pylon oscillation was encountered. The oscillation exhibited the following distinctive characteristics: low frequency (0.1–0.2 cycles/rotor revolution), limit cycle (±1–2 deg pylon motion, depending on speed), with the rotor and pylon whirling direction opposite that of rotor rotation. Pylon modifications, which in effect increased the pylon mounting stiffness, made testing possible to 160 knots with 20 deg of delta-three.

An extensive program of analyses and model testing was then begun to investigate the low-frequency rotor-pylon oscillation phenomenon. The objectives of those investigations were to provide a physical understanding of rotor-pylon stability, to develop an analytical treatment, and to establish means of assuring stable configurations for the XV-3 and future tilt-rotor VTOL designs. Both a simple closed-form analysis and a more complicated open-form digital analysis were developed.

Concurrently with these analyses a model program was initiated. Interaction between the analytical and dynamically scaled model work made possible the guiding of one program by the current data from the other. The dual approach also helped in the development of a physical understanding of rotor-pylon stability. By June 1965, an explanation for and means of eliminating the stability problem had been shown, at which time a full-scale test program was initiated. That program included analyses, inspection, modification, instrumentation, shake tests and, finally, wind-tunnel tests of the XV-3 tilt-rotor aircraft.

The tunnel tests were conducted in the NASA Ames 40- × 80-ft wind tunnel. The tests proceeded as planned with trends and actual stability characteristics essentially as predicted by prior analyses. With changes previously defined by the analyses, stability through tunnel maximum speed (192–197 knots) was demonstrated with several different configurations.

## Rotor-Pylon Behavior

A tilt-rotor VTOL incorporates wing-tip-mounted tilting pylon and rotor assemblies. In the case of the XV-3, the pylons are flexibly mounted for vibration isolation and have limited angular freedom in pitch and yaw. Rubber mounts and viscous dampers provide restraint for the pylons. It is obvious that for any decrease in damping to occur or for a sustained oscillation to develop, destabilizing forces must be generated by the rotor. Such forces are, in fact, generated by the rotor and at high inflow angles can become significant in determining the coupled rotor-pylon stability.

Figure 2 illustrates the forces acting on a rotor and pylon system during steady pitching motion. After the initial transient, the rotor follows the pylon at a precession rate equal to the pylon pitch rate ($\dot{\phi}_x$) and assumes the lagging condition shown, as discussed in Ref. 6. The flapping moment to precess the rotor results from cyclic lift changes, which are indicated by $\pm\Delta L$. The differential lift is a result of blade flapping relative to the rotor shaft. At high advance ratios and corresponding high inflow angles ($\phi_o$), the $\Delta L$ forces have components $\Delta T$ and $\Delta H$ as shown on the figure. The differential $\Delta T$ generates the flapping moment that precesses the rotor, and its reduction with inflow is responsible for the increased flapping. The $\Delta H$ components, both being in the same direction, add and thereby produce a hub shear force in the direction of the pylon pitching rate. That destabilizing moment has the average value,

$$M_H = I_b(\dot{\phi}_x + \dot{a}_1)\, Vh/\bar{R}^2$$

per blade. The destabilizing effect can be seen to be directly proportional to blade inertia, airspeed, mast length, and number of blades, and inversely proportional to rotor radius squared. Very important also is the relation between the magnitude and phase of the two variables, pylon rate ($\dot{\phi}_x$) and rotor flapping rate ($\dot{a}_1$). Factors that increase the rotor response rate include pitch-flap coupling and elastic flapping restraint. Both act to decrease the steady flapping (which was earlier noted to be a problem during maneuvers); however, the increase in rotor response rate is destabilizing. Flapping restraint has the advantage of producing an additional stabilizing aerodynamic moment for pylon motions, making its net effect stabilizing.

The spring-inertia components of the basic pylon cause its motion following a disturbance to be oscillatory. Conse-

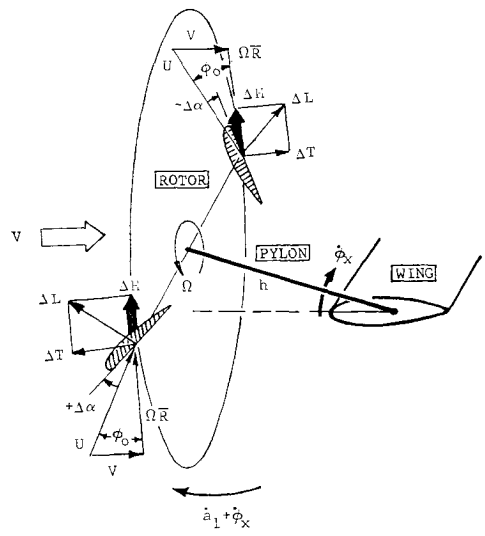


**Fig. 2 Rotor tip-path-plane schematic showing origin of destabilizing force.**

quently, it is useful to consider the effect of frequency on the destabilizing rotor force. Plotted on Fig. 3 is the destabilizing rotor force (with the rotor producing zero net thrust) as a function of the ratio of control axis frequency to rotor rpm. The force component in phase with pylon displacement (which acts as a negative spring) and the component in phase with pylon rate (which has the effect of negative damping) are both shown. First, consider the condition with no delta-three. At zero frequency the steady condition (Fig. 2) exists and the destabilizing rotor force acts as negative damping. By increasing the pylon (or control axis) frequency, the pylon begins to oscillate faster than the rotor can respond; finally, the rotor remains essentially fixed in space even though the pylon continues its motion. At that point, the destabilizing damping force approaches zero as is shown. With the rotor remaining fixed in space, flapping relative to the rotor shaft takes place and aerodynamic forces are generated which are maximum at maximum pylon displacement. The result is that the destabilizing rotor force acts as a negative spring for pylon motions at high frequencies.

From the foregoing, it can be seen that the effect of the rotor on the pylon is to produce negative damping, which is predominant at very low frequencies, and to introduce a negative spring term that is predominant at higher frequencies. Consequently, the effect of the basic rotor on pylon oscillations is to reduce both their damping and frequency.

The curves shown on Fig. 3 also illustrate the effect of delta-three. Because delta-three increases the rotor natural flapping frequency through its action as a flapping restraint, that frequency shifts from 1.0 per rev to 1.1–1.3 per rev in the rotating coordinate system depending on the magnitude of delta-three. That frequency corresponds to 0.1–0.3 per rev in the fixed system and is the cause of the peak shown on the damping curve with delta-three. Both with and without delta-three, pylon oscillations can be kept stable by setting the pylon frequency well above the rotor natural frequency, thereby minimizing the coupling effects and allowing the basic pylon damping to remain greater than the destabilizing contribution from the rotor.

Up to this point, the effect of the rotor on the pylon has been discussed. The effect on the pylon on the rotor is also very significant. Delta-three, flapping hinge offset, or elastic flapping restraint which is generally incorporated in rotors to reduce the steady-state flapping, all have the further effect of raising the natural flapping frequency to above 1.0 per rev, for example, to 1.2 per rev. Blade flapping at that frequency appears in the fixed coordinate system as a circular weaving of the tip-path plane at 0.2 per rev. When the pylon is not free to move, this rotor mode of motion is highly damped (70–90% of critical). Freeing the pylon introduces the possibility that the rotor mode can be unstable. The destabilizing rotor forces are strongly a function of inflow ratio. As the amplitude of the oscillation increases, the effective inflow is reduced and a limit-cycle situation exists.

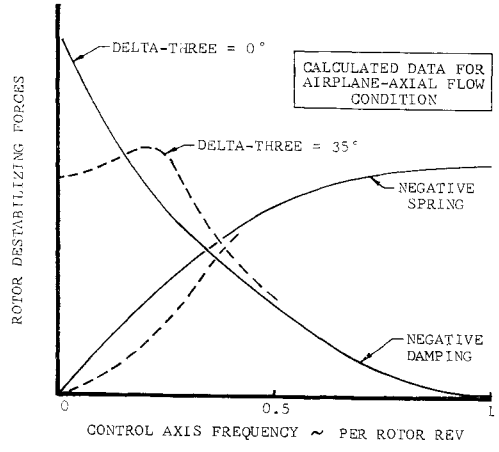


**Fig. 3 Rotor destabilizing force vs control axis frequency.**

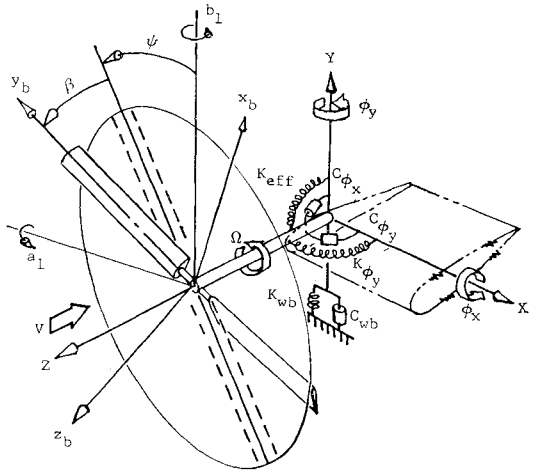


**Fig. 4 Mathematical model for two-bladed rotor.**

Pylon mounting stiffness is a primary parameter determining stability of the rotor mode. Equally effective is the isolation of the cyclic control system from pylon motions through the use of a control coupling arrangement. Pylon inertia and applied damping have little effect on rotor mode stability because of their small magnitude in relation to the rotor-generated forces.

## Analytical Investigations

Two analytical methods were developed to investigate the stability of rotor-pylon systems at high-inflow conditions.

### Linear Closed-Form Analysis

One of these methods is a linear closed-form analysis of a 4-degree-of-freedom rotor-pylon system. The tip-path-plane equations are derived using the flapping coordinates $a_1$ and $b_1$, and two pylon equations are derived using the pylon displacement coordinates $\phi_x$ and $\phi_y$. A mathematical model and coordinate system similar to the one used in this analysis is shown on Fig. 4.

The equations of motion for the rotor plane contain provisions for hub restraint, pitch-flap coupling, swashplate-pylon coupling about both pitch and yaw pylon axes, and swashplate phasing. Since the rotor equations of motion are written with respect to the tip-path-plane coordinates, the analysis can be applied easily to a rotor with any number of blades. The analysis also includes the effect of finite wing torsional and beamwise flexibility. Pylon-wing coupled modes are thereby considered along with over-all system stability. The analysis treats the vertical motion of the pylon support as an added degree of freedom of the basic 4-degree-of-freedom analysis. The wing torsional degree of freedom is treated as a finite wing stiffness in series with the pylon mount stiffness.

### Digital Open-Form Analysis

For the detailed analysis of a specific rotor-pylon configuration, a digital open-form analysis is used. The technique consists of a step-by-step numerical integration of the equations of motion of the rotor and pylon system. This method is discussed in detail in Ref. 6. References 7–9 present recent work in the related area of propeller-nacelle whirl flutter.

The basic two-bladed mathematical model for which equations are derived is shown in Fig. 4. The airloads are distributed over the blade in ten segments and include the effects of stall, compressibility, and tip loss. As in the linear analysis, the effects of hub restraint, delta-three, swashplate-pylon coupling, and swashplate phasing are considered. Wing

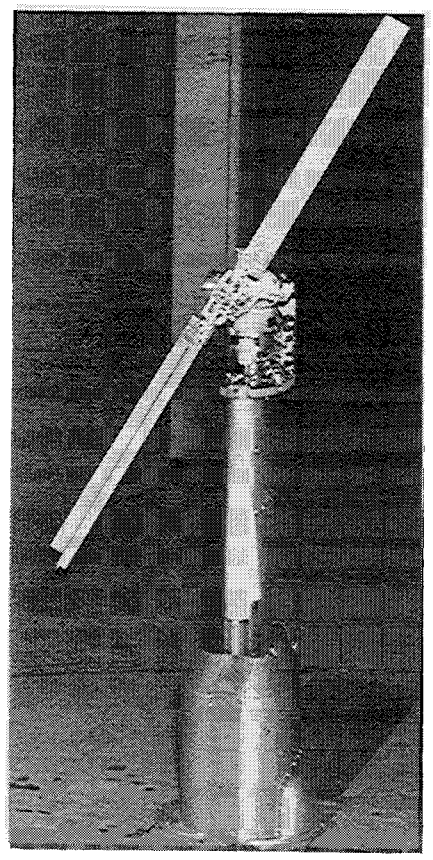

**Fig. 5 Dynamically scaled rotor-pylon-wing model in 7 × 10-ft tunnel.**

flexibility was included, using the wing parameters shown on Fig. 4. The wing torsional stiffness is assumed to act in series with the pylon mounting stiffness, while the wing bending is treated as a separate degree of freedom. The output of this analysis consists of a time history of the pylon and wing motions, from which the stability of the configuration is evaluated.

## Model Investigations

A powered, dynamically scaled model of the XV-3 rotor and pylon systems was constructed to determine fundamental modes of oscillation, controlling parameters for rotor-pylon stability, and the effect of various stabilizing devices. Following extensive testing of that model, a second model (Fig. 5) was fabricated to evaluate rotor-pylon stability at higher scaled speeds and to include the effects of wing flexibility on the pylon and rotor modes of motion.

The scaling of the models to preserve dynamic similarity included holding the following factors the same for model and for full scale: rotor Lock number, rotor solidity, rotor advance ratio, and pylon frequency ratio. The rotor rpm, which sets the time scale, was chosen primarily from hardware and maximum tunnel speed considerations, since neither Mach number, Reynolds number, nor gravity effects were scaled. Although no detailed attempt was made to scale the blade flexibility in either model, the fundamental blade modes in the second model were very near scale. Blade flexibility does involve intrinsic dynamic considerations that are of importance; however, analytical and experimental work conducted during this investigation has shown it to have little effect on the basic rotor-pylon stability modes under discussion.

The models were designed to allow wide variations of as many parameters as possible. Pylon stiffness and damping, control system coupling, and rotor pitch-flap coupling were readily adjustable. Testing was conducted in the axial-flow flight condition (airplane cruise mode for the tilt-rotor VTOL). The common objectives and the close relation between the model and analytical investigations make it advantageous to discuss results of these programs together.

## Analytical and Model Results

The objectives of the analytical and model programs were to simulate the instability encountered by the XV-3 during the 1962 wind-tunnel tests, to isolate the major parameters affecting that instability, and to develop means of eliminating or controlling the problem. At the conclusion of the effort, the objectives had been realized.

### Simulation of Instability

As has been discussed, the characteristics of the instability encountered included limit-cycle oscillation of about 0.1–0.2 per rev with the rotor and pylon precessing against the direction of rotor rotation. Figure 6 illustrates the simulation of the full-scale instability by model and analytical means. Rotor flapping, pylon pitch and yaw positions, and rotor azimuth traces are shown for all systems, except for the yaw position of the full scale, which was inoperative. Figure 6a shows the limit-cycle oscillation as recorded during the full-scale tests near 130 knots; Fig. 6b, from the dynamically scaled model; and Fig. 6c from the computer. Simulation of the limit-cycle oscillation by the model and the computer is apparent, with a retrograde precession at a subharmonic frequency being present in each case. Minor frequency differences between the model-computer and the full scale result from the difficulty of obtaining parameter values for the full scale with sufficient accuracy to duplicate exact frequency and damping characteristics. Note the nearly exact agreement between the model and computer, where the parameters are well defined.

### Effect of Major Parameters

In investigating the effect of various parameters, it became clear that rotor-pylon oscillations generally fall into two categories, either near the pylon or the rotor natural flapping frequency. Hence, the terms pylon mode and rotor mode are used to describe those oscillations.

In the pylon mode, the oscillation takes place near pylon natural frequency and the rotor remains essentially fixed in space. Pylon oscillation at a low frequency, from 0.1 to 0.3 per rev, is characteristic of the rotor mode, and rotor flapping

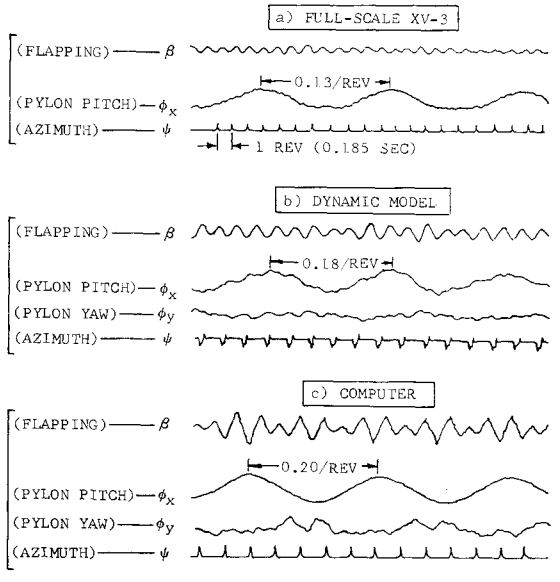


**Fig. 6 Model and computer simulation of XV-3 rotor-pylon limit cycle oscillation.**

in space is also large. Depending on the parameters used, each mode can occur in a forward or backward whirl direction with respect to rotor rotation. For the range of values typical of the XV-3, the rotor and pylon modes are both backward whirl modes. The effect of parameter changes on each of these modes is quite different; only minor levels of pylon damping are required to maintain stable oscillation in the pylon mode, while pylon damping has little effect on the low-frequency rotor mode. Since only the backward whirl rotor mode was encountered by the XV-3, and since all indications have been that typical rotor-pylon systems designed for tilt-rotor VTOL are more susceptible to unstable rotor rather than unstable pylon modes, this study has concentrated on the rotor mode. Consequently, the following discussions based on the model and analytical results relate to the low-frequency rotor mode.

### *Pylon mounting stiffness*

A major parameter determining rotor-pylon stability was shown to be the pylon mounting stiffness. The destabilizing inplane rotor spring force must be reacted by the pylon spring. As pylon spring rate is increased, pylon oscillations are sufficiently rapid that the rotor cannot follow and the rotor mode of oscillation remains highly damped. Because the rotor forces become more destabilizing as speed (inflow) is increased, there is always a speed at which the basic system will become unstable. Increases in pylon stiffness can extend that speed to a point well beyond the maximum speed capability for the typical tilt-rotor VTOL.

### *Swashplate-pylon coupling*

Angular motion of the pylon results in an equal change in cyclic blade feathering with respect to the reference axis if blade control is locked to the pylon. The angular motion of the control axis disturbs the rotor plane and destabilizing rotor forces are generated. A simple and effective method of assuring rotor-pylon stability is the isolation of control axis motions from pylon motions by swashplate-pylon displacement coupling. Figure 7 illustrates such a coupling system. A mechanical parallelogram linkage holds the swashplate fixed with respect to the wing during displacements of the pylon. For a rotor having no delta-three or elastic flapping restraint, the system shown isolates the rotor from the pylon for angular motions. The coupling ratio ($K_x$) shown is defined as $+1$. With delta-three, an increase in coupling is required. Studies have indicated that values near $+1.5$ to $+2$ are near optimum for the XV-3. The azimuth phase angle between swashplate motions and pylon motion (retardation angle) is an integral

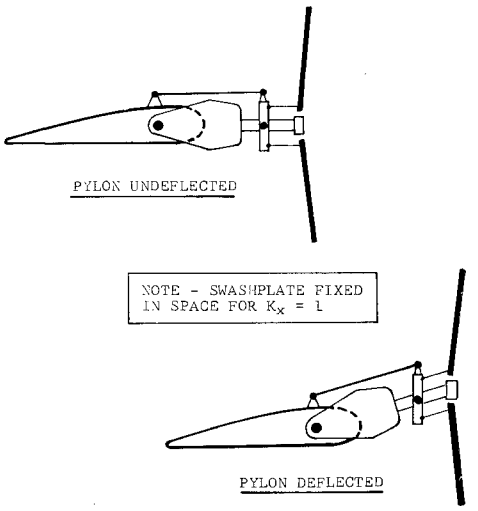


**Fig. 7 Schematic illustrating swashplate-pylon coupling.**

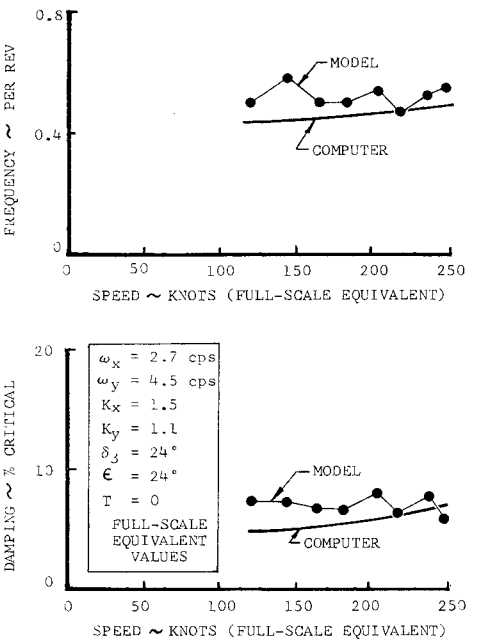


**Fig. 8 Rotor-pylon stability with swashplate-pylon coupling and increased pylon stiffness—model and computed data.**

part of control coupling. For a rotor having delta-three, pitch and yaw motions are coupled. Using a retardation angle equal to the delta-three angle has been demonstrated to minimize that cross-coupling.

Model and computer data for the XV-3 with swashplate-pylon coupling and with increased pylon stiffness are shown on Fig. 8. The frequency and damping characteristics of pylon motion following a test disturbance are shown as a function of equivalent full-scale speed. There was no indication from the model of a low-frequency mode through the maximum speed tested (~250 knots) and computer results display the same trend. By comparison with the limit-cycle case at 130 knots (Fig. 6), it is seen that the indicated parameter changes are strongly stabilizing.

### *Delta-three*

The use of rotor delta-three to control steady and maneuver-induced rotor flapping generally entails a reduction in the speed for neutral rotor-pylon stability unless other factors are modified. This is because the rotor flapping natural frequency is increased by the equivalent flapping spring effect of delta-three. As a consequence, higher pylon natural frequency is required to avoid undesirable coupling of the pylon with rotor motions. Because the rotor flapping natural frequency is also a function of inflow condition, the effect of delta-three is also dependent on forward speed. Both the model and analytical work showed that below about 150 knots for the XV-3, delta-three has little effect; at higher speeds it becomes destabilizing.

### *Rotor elastic flapping restraint*

Spring restraint on rotor flapping was shown to be stabilizing on the model. Analytical methods likewise predict an increase in stability. Although flapping restraint increases the rotor response rate, which is destabilizing, it introduces moments to the pylon out of phase with pylon rate sufficiently large to increase the over-all system damping.

### *Wing effect*

For each of the conditions investigated in which a rotor mode instability was present, releasing the wing beam and tor-

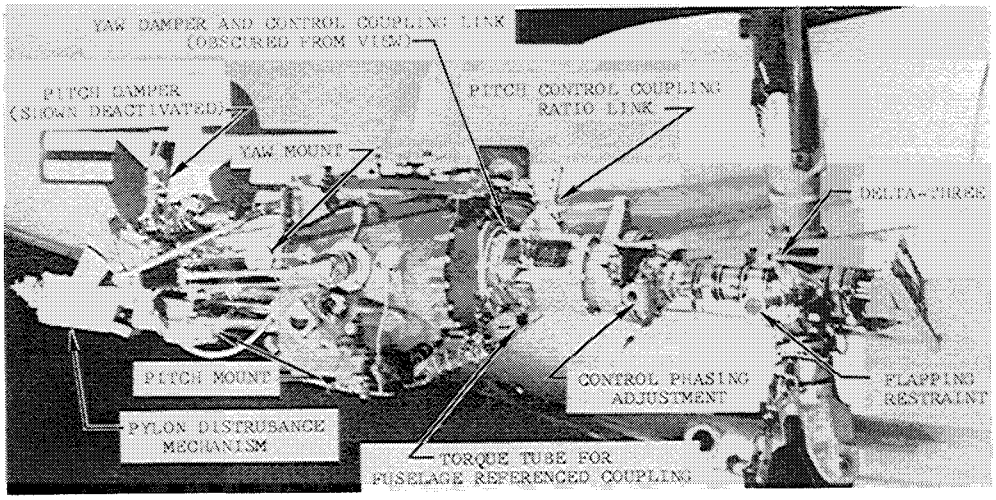


**Fig. 9 Test parameters, XV-3 full-scale tunnel tests.**

sional degrees of freedom, or including their effect in the analysis, reduced the speed at which the mode became neutrally damped. The reduction in speed for neutral damping was on the order of 20 knots or less (full-scale). The principal mechanism of the reduction is related to the pylon frequency, which is lowered by the wing freedom.

## Full-Scale Wind-Tunnel Tests

Arrangements were made with NASA for Bell Helicopter Company to modify the XV-3 in preparation for joint NASA-Bell testing in the NASA Ames 40- × 80-ft tunnel. The overall objective of the test was to generate stability data for correlation with the analytical and model work that has been discussed.

### Aircraft Modification

Modifications were made to the XV-3 to permit rapid variation in each of the system parameters that had been shown by the preceding work to have a significant effect on rotor-pylon stability. These modifications included provisions to change the swashplate-pylon control coupling in pitch and yaw, control phasing (retardation), pylon mounting stiffness and damping in pitch and yaw, rotor flapping restraint, and rotor pitch-flap coupling. A bearing-mounted torque tube was installed inside the wing to provide a fuselage reference for the pitch swashplate-pylon coupling. When using that reference, wing torsional effects were minimized. A hydromechanical pylon disturbance device was installed on the right wing tip for generating a test disturbance to the rotor-pylon system to aid in establishing the stability level before the neutral stability point was reached. A side view of the right-hand pylon of the XV-3 following modification for testing is shown on Fig. 9.

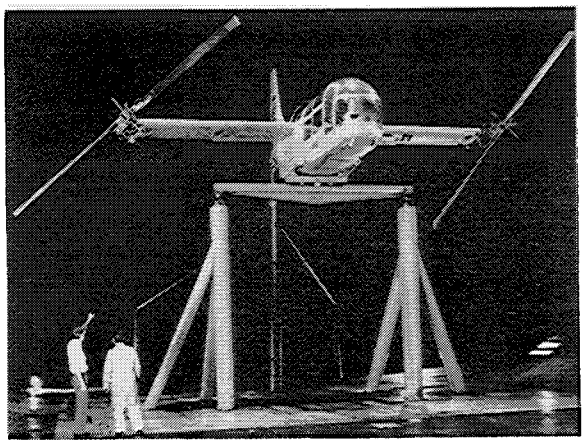

**Fig. 10 XV-3 in NASA Ames 40- × 80-ft tunnel—roll freedom mounting.**

In addition to the modifications made to the pylon-rotor system, a tunnel mounting system that allowed the aircraft to have limited freedom (±3 deg) in roll was designed and fabricated. Roll freedom was introduced to more nearly simulate the free-flight condition. Thus, the wing was restrained only by the fuselage. Rubber mounts provided a low, but positive, roll spring rate.

### Test Installation

The XV-3 was first mounted in the tunnel using a conventional three-support mounting. One support was attached to the aft end of the fuselage and the other two supports were attached to the wings near the node points for the first wing beam bending mode. In addition to the wing-mount system just described, the roll-freedom mounting system shown on Fig. 10 was used for a second series of tests. A remote control console provided complete control of the aircraft from outside the tunnel.

### Test Methods

Because of the potentially hazardous nature of the testing, considerable attention was given to developing a test procedure that would avoid highly unstable conditions. To obtain stability data with a given configuration, tunnel speed was first set to 60–70 knots and rotor thrust trimmed to 0 for minimum stability. With trim established, the pylon was disturbed by the test device shown on Fig. 9. The pylon motion traces, being directly available from the oscillograph, were immediately analyzed for damping level and frequency content. This information was plotted over computer-calculated data for the specific configuration being tested, and the two were compared. Depending on the trend of damping and/or frequency exhibited by the rotor-pylon configurations being tested, a decision was made about increasing tunnel speed and continuing the test. Thus, it was possible to proceed to the point of neutral stability with minimum risk. For a number of configurations, the testing was terminated before the neutral damping speed was reached, to reduce the risk further.

## Test Results and Correlation

Sixteen configurations of the basic rotor-pylon system were evaluated during the course of 25 runs. The following summarizes the results: 1) Rotor-pylon stability was essentially as predicted at tunnel maximum speed using stabilizing parameters (maximum speed 192–197 knots). 2)Rotor-pylon instability was demonstrated at low speed using destabilizing parameters (neutral stability at ~100 knots). 3) 1962 test results were rechecked (indications of low-frequency mode at

164 knots; prior testing was not extended past 160 knots with best stiffened pylon configuration because of indications of the low-frequency mode and because of tunnel operational considerations). 4) Parameter effects were verified (consistent with model and theoretical investigations). 5) Rotor characteristics were checked (delta-three and flapping restraint confirmed to reduce flapping; propulsive efficiency in excess of 80% at design speed with reduction at higher speeds was not as severe as indicated by previous extrapolations.[5])

### Summary of Stabilized Configurations

Three configurations that had been predicted by the theoretical and model work to be stable to speeds in excess of those obtainable in the 40- × 80-ft tunnel were tested at maximum tunnel speed and did demonstrate highly stable rotor-pylon behavior at those speeds. Table 1 indicates the parameter values of each configuration. Note that there is a progression from a stiff pylon system having swashplate coupling in pitch and yaw (pitch coupling on the first configuration shown was fuselage-based through the wing torque-tube arrangement) with low delta-three and with flapping restraint, to a simplified configuration having low pylon pitch frequencies, no coupling (or damper) in yaw, high delta-three and no flapping restraint. In addition, the latter configuration was tested using the roll-freedom mounting system while the other two were mounted on the wings.

### Demonstration of Instability

Rotor-pylon instability was demonstrated at a tunnel speed of 96 knots by reducing the pylon frequency in pitch to near 2.5 cps and in yaw to 3.8; introducing destabilizing (−0.5 deg/deg) swashplate coupling in pitch and yaw; and removing the flapping restraint. The oscillation frequency was just under 0.2 cycles per rev at the low damping point. The oscillation also exhibited backward whirl and considerable rotor flapping which is characteristic of the rotor mode. This destabilized configuration provided a baseline for illustrating the effect of specific parameter changes.

### Recheck of 1962 Test Results

With the XV-3 configured as nearly as possible as it was for the best stiffened pylon run of the 1962 investigation, and with the swashplate essentially locked to the mast as was the case in 1962, testing was conducted through 164 knots before an indication of rotor mode oscillation was present. This compares favorably with the speed of 160 knots which was the highest speed tested in 1962 because of indications of reduced damping in the low-frequency mode and because of tunnel operational considerations at that speed. The absence of swashplate-pylon coupling is the primary factor allowing the mode to degenerate. The 130-knot instability conditions experienced during the 1962 tests, with the pylon dampers set to minimize their spring effect, were also simulated during the subject testing. During that simulation, instability occurred at 125 knots. Since the aircraft was mounted on the roll-freedom system during the case being cited, the 5-knot difference is reasonable. It can therefore be concluded that the miscellaneous changes to the control system and wing structure that were made to improve their operation had no major effect on rotor-pylon stability.

**Table 1 Stabilized configuration summary**

| Configuration | 2 | 7 | 21C |
|---|---|---|---|
| Tunnel mount | Wing | Wing | Roll free |
| Pylon frequency pitch/yaw, cps | 3.4/6.6 | 3.4/3.5 | 2.5/5.7 (yaw damper off) |
| Swashplate coupling pitch/yaw | [1]Fuselage/[1] | 1/1 | 1.5/0 |
| Delta-three, deg | 22 | 22 | 35 |
| Flapping restraint, in.-lb/deg | 740 | 0 | 0 |
| Maximum test speed (tunnel max.), knots | 193 | 197 | 192 |

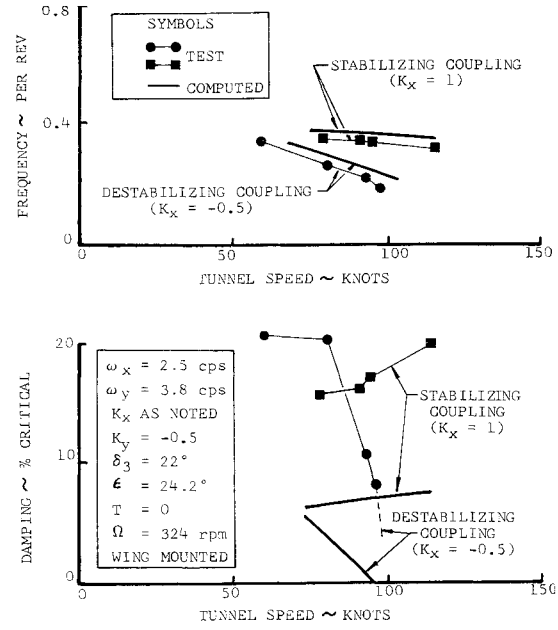


**Fig. 11 Effect of swashplate-pylon coupling—XV-3 tunnel test and computed data.**

### Parameter Effects

The major parameter effects on the full-scale XV-3 were determined experimentally by making successive runs in which only the parameter under study was changed.

#### *Swashplate-pylon coupling*

The strongly stabilizing effect of swashplate-pylon coupling was demonstrated in a series of runs involving both soft and stiff pylon configurations and during the wing-mounted and roll-freedom tests. Configuration 7, which was discussed earlier as being highly stable through maximum tunnel speed, was essentially the basic XV-3 system but with control coupling in pitch and yaw. Shown on Fig. 11 are the frequency and damping data from two configurations differing only in the amount of swashplate-pylon pitch coupling. The stabilized swashplate configuration ($K_x$ = 1) is highly stable, while the destabilized coupling ($K_x$ = −0.5) of the baseline case causes instability near 100 knots. With the stabilizing coupling, there is no major decrease in rotor-pylon frequency. The computer calculations for rotor-pylon systems equivalent to those being tested are also shown on Fig. 11. The frequencies correlate exactly with respect to mode shape (rotor or pylon mode) and very well quantitatively, although the calculated frequencies are slightly higher than test values. Excellent correlation exists between predicted and test speeds for neutral damping. Predicted damping levels are conservative (low) at points away from neutral stability as compared to the experimentally observed values.

#### *Pylon stiffness*

Increased pylon stiffness was configured to be a stabilizing factor. Figure 12 illustrates two runs, one made with a low pitch frequency (2.5 cps) which is the baseline case, the other with an increased frequency (3.4 cps). In the lower-frequency case, the rotor mode is entered just below 100 knots. With in-

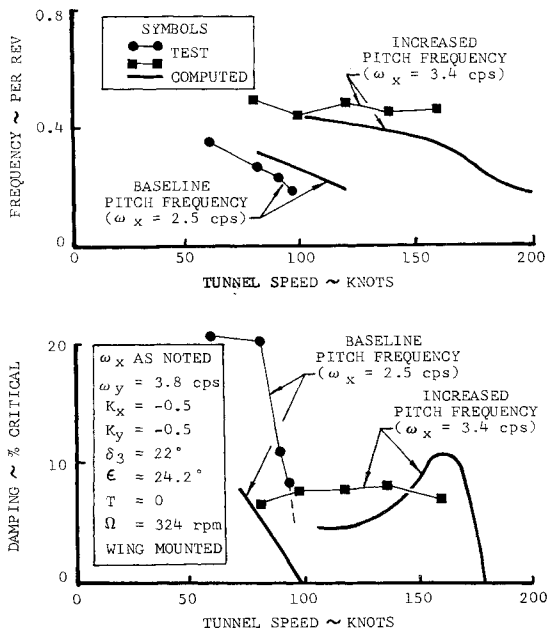


**Fig. 12 Effect of pylon frequency—XV-3 tunnel test and computed data.**

creased stiffness, oscillations following the test disturbance occur near pylon frequency up to about 160 knots, where the first indications of a low-frequency mode appear. The increased pylon frequency keeps the rotor and pylon frequencies separated up to that point so that stability is maintained. For both test cases destabilizing swashplate-pylon coupling was used to reduce the stability to a measurable value at a low test speed for comparison purposes. The computer data can be seen to correspond closely to the test data.

### *Rotor flapping restraint*

As predicted by theory and demonstrated by model tests, rotor flapping restraint on the full-scale XV-3 markedly increased rotor-pylon stability. The magnitude of the flapping restraint that was used (740 in.-lb/deg/blade) was sufficient to raise the rotational flapping natural frequency $\omega_\beta/\Omega$ to 1.17 per rev. This is within the optimum band of 1.1 to 1.2 per rev that is discussed in Ref. 10. Test data from the baseline case (low pylon frequency, destabilizing coupling and no flapping restraint) are compared with data from that same configuration but having flapping restraint as shown on Fig. 13. The oscillation frequency was maintained to a higher speed and the damping did not experience significant reduction until about 120 knots, at which point testing was discontinued. Extrapolation of the damping data indicates a neutral damping speed of about 140 knots. Similarly, the computer calculations showed 140 knots to be the neutral damping speed. The flapping restraint also had a major effect on flapping amplitude, as will be discussed later.

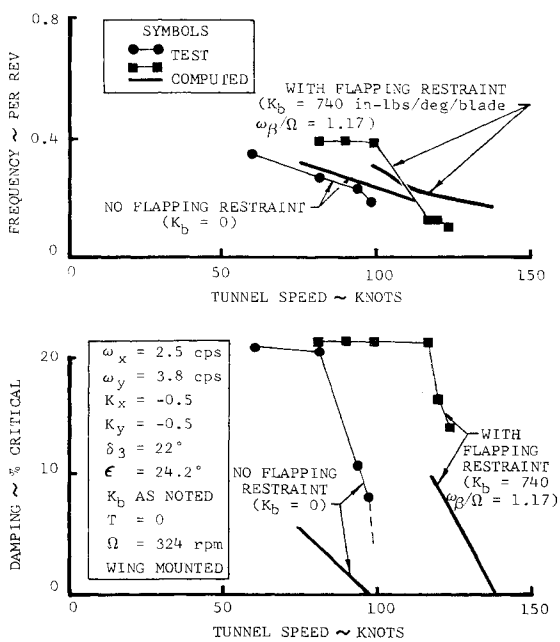


**Fig. 13 Effect of rotor flapping restraint—XV-3 tunnel test and computed data.**

### *Delta-three and tunnel mounting*

As predicted by theory, little effect on stability was noted when delta-three was increased from 22 to 35 deg when the low pylon frequency allowed neutral stability to occur near 100 knots. Stable operation at high speeds with 35-deg delta-three was demonstrated; however, no attempt was made to demonstrate the predicted destabilizing effect of delta-three at higher speeds for the safety reasons mentioned earlier. The slightly (~5 knots) destabilizing effect of roll freedom was shown during two sequential runs, one with the wing mount and one with the roll-freedom mount. The reduction in wing beamwise frequency is a primary factor in lowering the stability through its effect on the first pylon-wing mode frequency, although the existence of roll as a separate degree of freedom also makes possible other coupling effects. Runs at higher speeds with roll freedom indicate that roll damping can decrease as the rotor mode approaches low damping; however, there was no case in which the roll mode exhibited instability.

### Correlation Summary

A summary of the correlation between the full-scale and computer data is shown on Fig. 14. Of primary importance is the relationship between actual and computed neutral damping speeds because it is that speed which must be extended by design well beyond the flight speed range in an operational tilt-rotor VTOL aircraft. Figure 14a shows the good agreement between test and theory for all the runs that were taken to the

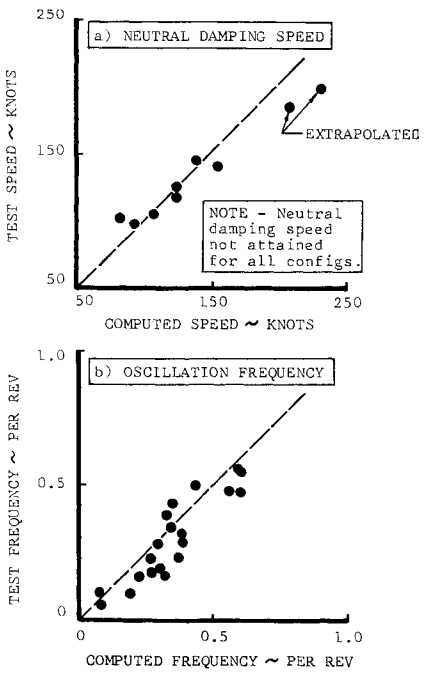


**Fig. 14 Correlation summary—tunnel test and computed data.**

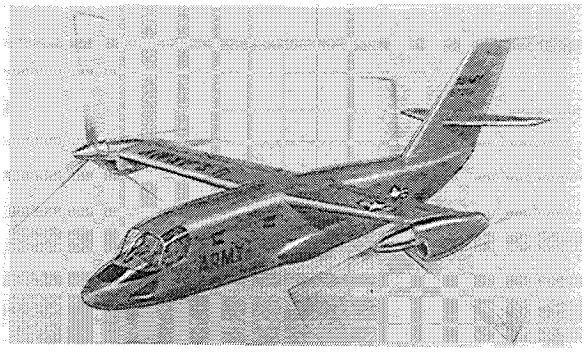

**Fig. 15 A 300–400-knot 28,000-lb tilt-rotor VTOL.**

neutral damping speed. For lower speeds, the measured damping is higher than predicted. Figure 14b shows the correlation between the computed and test values of mode frequency. Points are plotted both for the highest speed and lowest speed of each run. A number of runs are not included because the damping was so high that frequencies were not measurable.

### Rotor Characteristics

Rotor flapping with aircraft angle of attack, and the rotor propulsive efficiency were briefly checked. A comparison of the flapping slope (change in flapping amplitude per unit angle-of-attack change) at 140 knots illustrates the effect of delta-three and flapping restraint. Basing the comparison on the 22-deg delta-three case with no flapping restraint, it was found that with 35-deg delta-three, the slope was reduced to 65% of the baseline value; with 22-deg delta-three and flapping restraint (740 in.-lb/deg/blade) the reduction was to 55% of the zero flapping restraint value. That result confirms the usefulness of these two parameters in controlling rotor flapping during maneuvers. Proprotor propulsive efficiency was checked during certain of the runs to establish trends of efficiency variation with speed. Earlier data[5] had shown that a propulsive efficiency in excess of 80% could be realized. Exptrapolation of those data to speeds well beyond the design point indicated a considerable reduction in efficiency with speed. Actual test data obtained during the latest testing up to maximum tunnel speed showed that the drop in efficiency was less severe than indicated by the extrapolations.

## Conclusions

From the results of these investigations of tilt-rotor VTOL aircraft rotor-pylon stability, the following is concluded:

1) A tilt-rotor VTOL having stable rotor-pylon characteristics during high-speed operation can be designed.

2) Analytical and model predictions of rotor-pylon stability characteristics for future higher-speed designs are valid.

3) Simple mechanical means are available and have been demonstrated to provide rotor-pylon stability. These include swashplate-pylon displacement coupling, pylon mounting stiffness increase, and rotor elastic flapping restraint.

Although an understanding of and a solution to rotor-pylon stability problems have been established, work continues on refining the analytical and model techniques for future tilt-rotor VTOL aircraft designs. Such an aircraft is shown on Fig. 15. The dynamic model shown on Fig. 16 is an aeroelastically scaled model of that aircraft design. The scaling includes maintaining distributed stiffness and mass characteristics of all major components such as the blades and wing. Stable operation through speeds near 500 knots has been demonstrated with this model. From the background of these investigations and prior flight programs, it is now known that tilt-rotor VTOL aircraft can be developed that hover efficiently and attain high cruise speeds with good flight characteristics and low vibration levels.

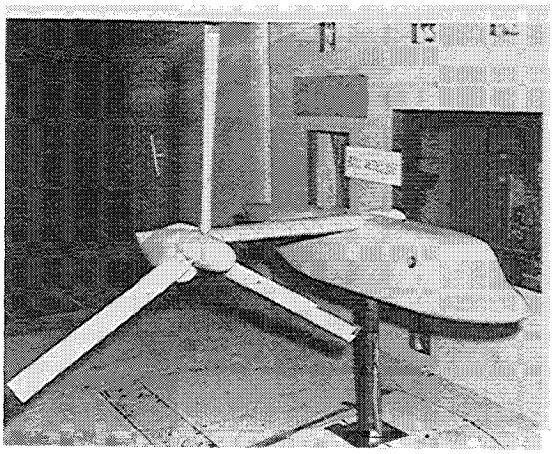

**Fig. 16 An aeroelastically scaled dynamic model of a tilt-rotor VTOL.**

## References

[1] Leibensberger, C. E., "Phase I Flight Test Results of the XV-3," Rept. 200-099-928, Oct. 1958, Bell Helicopter Co.

[2] Deckert, W. H. and Ferry, R. G., "Limited Flight Evaluation of the XV-3 Aircraft," TR-60-4, May 1960, Air Force Flight Test Center.

[3] Drinkwater, F. J., III, "Operation Technique for Transition of Several Types of V/STOL Aircraft," TND-774, March 1961, NASA.

[4] Quigley, H. C. and Koenig, D. G., "The Effect of Blade Flapping on the Dynamic Stability of a Tilting-Rotor Convertiplane," TND-778, April 1961, NASA.

[5] Koenig, D. G., Grief, R. K., and Kelly, M. W., "Full-Scale Wind-Tunnel Investigation of the Longitudinal Characteristics of a Tilting-Rotor Convertiplane," TN D-35, Dec. 1959, NASA.

[6] Hall, W. E., Jr., "Prop-Rotor Stability at High Advance Ratios," *Journal of the American Helicopter Society*, June 1966.

[7] Houbolt, J. C. and Reed, W. H., III, "Propeller-Nacelle Whirl Flutter," *Journal of the Aeronautical Sciences*, Vol. 29, No. 3, March 1962, pp. 333–346.

[8] Richardson, J. R. and Naylor, H. F. W., "Whirl Flutter of Propellers with Hinged Blades," Rept. 24, March 1962, Engineering Research Associates, Toronto, Canada.

[9] Reed, W. H., III, "Propeller-Rotor Whirl Flutter, a State of the Art Review," presented at the Symposium of the Noise and Loading Actions on Helicopter V/STOL Aircraft and Ground Effect Machines, Southampton, England, Aug 30–Sept. 3, 1965.

[10] Young, M. I. and Lytwyn, R. T., "The Influence of Blade Flapping Restraint on the Dynamic Stability of Low Disc Loading Propeller-Rotors," Paper 132, May 1967, American Helicopter Society, New York.